Research Square

Preprints are preliminary reports that have not undergone peer review.
They should not be considered conclusive, used to inform clinical practice,
or referenced by the media as validated information.

LncRNA KCNQ10T1 shuttled by bone marrow mesenchymal stem cells-derived exosome inhibits sepsis via regulation of miR-154-3p/RNF19A axis

Haojie Yuan
Affiliated Hospital of Nantong University
Junbo Yu
Affiliated Hospital of Nantong University
Chun Liu
Affiliated Hospital of Nantong University
Jiajia Liu
Affiliated Hospital of Nantong University
Jianhua Xue
Affiliated Hospital of Nantong University
Heyan Zhao
Medical School of Nantong University
Yang Yang (Yangyang286228@ntu.edu.cn)
Affiliated Hospital of Nantong University

Research Article

Keywords: Sepsis, Long non-coding RNA, KCNQ1 Opposite strand/antisense transcript 1, MiR-154-3p, RNF19A

Posted Date: April 8th, 2022

DOI: https://doi.org/10.21203/rs.3.rs-1517198/v1

License: This work is licensed under a Creative Commons Attribution 4.0 International License.
Read Full License

Abstract

Objective

This study aims to discuss the role of exosomes KCNQ10T1 derived from bone marrow mesenchymal stem cells (BMMSCs) in sepsis, and to further investigate its potential molecular mechanisms.

Methods

Exosomes extracted from BMMSCs are identified by transmission electron microscopy (TEM), nanoparticle tracking analysis (NTA) and western blot. Fluorescence labeling is applied to detect the internalization of exosomes in receptors. The proliferation ability, migration ability and invasion ability of HUVECs are determined by CCK-8, EdU, wound healing and Transwell. The levels of inflammatory cytokines in sepsis cells are quantitatively detected by ELISA. Kaplan-Meier survival curve is used to describe the overall survival. RT-qPCR is used to detect mRNA expression of related genes. Bioinformatics analysis is performed to search the downstream target of KCNQ1OT1 and miR-154-3p and the interaction is verified by luciferase reporter assay.

Results

Exosomes derived from BMMSCs alleviated the toxicity in sepsis cell models and animal models. In mice with septic cell models, exosomal KCNQ10T1 was down-regulated and associated with lower survival. Overexpression of KCNQ10T1 inhibited the proliferation and metastasis of LPS-induced HUVECs. Further research illustrated that miR-154-3p was the downstream target gene of KCNQ1OT1 and RNF19A was the downstream target gene of miR-154-3p. Importantly, functional research findings indicated that KCNQ1OT1 regulated sepsis progression by targeting miR-154-3p/RNF19A axis.

Conclusion

Our study demonstrates that the exosomal KCNQ1OT1 suppresses sepsis via mediating miR-154-3p/RNF19A, which provides a latent target for sepsis treatment.

Introduction

Sepsis is a syndrome in which the human body causes an excessive response to various infectious diseases. Patients with sepsis show a series of symptoms such as high fever, nausea, vomiting, and even shock [1]. If sepsis cannot be treated in a timely and effective manner, it can lead to multiple organ dysfunction and severe diseases in the most severe cases, and it is also accompanied by severe immune dysfunction and catabolism [2]. In China, the incidence of sepsis is on the rise, and the sepsis-related deaths is also quite high [3]. Currently, the therapeutic strategies of sepsis are mainly antimicrobial therapy and fluid resuscitation therapy. However, most of clinical trials using antimicrobial drugs are failed in improving survival in patients with sepsis, and fluid overload can be detrimental to the heart [4, 5]. Therefore, it was urgent to explore new treatments for sepsis.

Bone marrow mesenchymal stem cells (BMMSC) have self-renewal and multidirectional differentiation potential. Therefore, the therapeutic potential of BMMSC for a variety of diseases has been deeply investigated [6, 7]. In addition, BMMSC has also been shown to interact with immune cells and participate in immune regulation [8]. Based on this immunomodulatory potential, it has been proposed that the therapeutic potential of BMMSCs is usually based on paracrine rather than cell-dependent approaches [9]. In recent years, it has become increasingly obvious that the therapeutic active ingredient of BMMSC is not only soluble factors, but vesicle structures-exosomes [10]. Exosomes are endogenous structures and secreted into the extracellular space. In the extracellular environment, these functional biomolecules are stably protected from external degrading enzymes through the lipid bilayer of the exosome membrane to mediate cell-to-cell microcommunication, immune regulation, and tissue regeneration [11]. Therefore, exosomes played an important role in transferring proteomic and genetic information levels to target cells.

Long non-coding RNAs (lncRNAs) are transcripts containing over 200 nt unable to encode proteins [12]. Studies have shown that abnormal expression of lncRNA is associated with the occurrence of many diseases, including sepsis [13]. Besides, increasing evidences have shown that lncRNAs are used as therapeutic targets for sepsis. For example, Wu *et al*. have depicted that lncRNA-HOTAIR facilitates the production of TNF-α in LPS-induced cardiomyocytes of mice with sepsis [14]. Yong *et al.* have revealed that in sepsis, lncRNA-MALAT1 reduces BRCA1 expression by targeting EZH2, thereby accelerating skeletal muscle cell apoptosis and inflammation [3]. KCNQ1 opposite strand/antisense transcript 1 (KCNQ1OT1) is located at 11p15.5 of KCNQ1 and is 91kb in length [15], and it has been proved to be closely related to the occurrence of many diseases. For example, lowering the level of KCNQ1OT1 alleviates myocardial I/R damage after acute myocardial infarction [16]. KCNQ1OT1 interacts with miR-140-5p to promote cholangiocarcinoma cell behavior, such as proliferation, migration and invasion [17]. However, the biological function of KCNQ1OT1 in sepsis had not been fully explored, and its exact molecular mechanism needed to be further elucidated.

Herein, we expect to investigate the involvement of lncRNAs and miRNAs in sepsis. It was speculated that exosomal KCNQ1OT1 might play a vital role in the progression of sepsis by targeting the miR-154-3p/RNF19A axis

Materials And Methods

Animals and groups

A total of 18 Male C57BL/6 mice, weighing 180–250 g were randomly divided into three groups: I) Control group (n = 6), treatment with saline; II) cecal ligation puncture group (n = 6, CLP), underwent CLP surgery;

III) Exosome group (n = 6, Exos), after CLP surgery, the mice were treated with exosome.

Cecal ligation puncture (CLP)

Sepsis animal model was established by CLP surgery. Before surgery, the C57BL/6 mice were anesthetized with ketamine (50 mg/kg) and xylazine (5 mg/kg). After disinfection, a midline incision was made in the abdomen. The cecum was then sectioned externally, ligated distally, and punctured once with a size 21 needle. Finally, the mice were resuscitated with saline.

Cell culture and treatments

BMMSCs were isolated from the red blood cells. In short, the red blood cells were first processed in the order of lysis, washing, re-suspension and culture. Then, the extracted cells are then purified and identified. Human Umbilical Vein Endothelial Cells (HUVECs) were obtained from American Type Culture Collection and mouse aortic endothelial primary cells were obtained from CLP model mice. All cells are cultured in an environment with room temperature and saturated humidity.

Isolation of exosomes

Exosomes were extracted from the supernatant of BMMSCs by ultracentrifugation. Briefly, the supernatant was filtered with SteritopTM 0.22 m sterile membrane, and then centrifuged at 100,000×g for 1.5 h. Subsequently, the precipitate was then re-suspended at PBS and centrifuged until the final volume was reduced to about 300 μL. Finally, the purified exosomes were stored − 80°C for later use.

Observation of exosomes by Transmission Electron Microscopy (TEM)

First, the purified exosomes were stained with 2% sodium phosphowolframate for 15 min, and then washed with PBS. Dried for 0.5 h at room temperature, exosomes were stained with 1% uranyl acid and observed using a TEM (Hitachi H7500 TEM, Tokyo).

Nanoparticle tracking analysis (NTA)

The size distribution and concentration of the isolated exosomes were detected by NanoSight LM10. First, exosome was dilute to 10000 times with PBS and mix upside down. Then, the diluted exosome was tested, photographed and recorded under professional guidance.

Western blot

The target cell protein was obtained by RIPA method, and the protein concentration was determined by BCA kit. Then, 50 ug prepared protein was taken for gel electrophoresis separation, and the isolated protein was electrically transferred to PVDF membrane (Roche, Switzerland). After blocked with 5% nonfat dry milk, the PVDF membrane was subjected to incubation with primary antibodies: CD63 (1:1000, ab134045, Abcam), CD9 (1:1000, ab92726, Abcam), HSP70 (1:1000, ab2787, Abcam) and VEGF (1:1000, ab32152, Abcam) at 4°C overnight. On the following day, the membrane was incubated with the secondary antibody at 37°C for 45 min. After washing the membrane film with TBST, luminescent solution was added and exposed in the gel imaging system. The protein content was analyzed using Quantity-One software.

Bioinformatics

StarBase (http://starbase.sysu.edu.cn/) was applied to speculate the target regulated by KCNQ10T1. miRwalk (http://www.umm.uni-heidelberg.de/apps/zmf/mirwalk/index.html), miRDB (http://www.mirdb.org/) and ENCORI (http://starbase.sysu.edu.cn/panCancer.php) were applied to predict the target genes regulated by KCNQ10T1 and miR-154-3p.

Fluorescence labeling

Follow the instructions of the PKH26 Red Fluorescent Cell Linker Mini Kit, the purified exosomes were labeled under dark conditions. After 24 h of culture, PKH26 were co-cultured with HUVECs. Then, the labeled exosomes were detected by immunofluorescence assay.

Cell Counting Kit-8

In brief, the cells adjusted to the appropriate concentration were inoculated on 96-well plates and treated accordingly. Next, each well was added with CCK-8 solution and incubated for 2 h in the dark. Finally, the absorption value at 450nm was measured by a microplate reader (Rayto, RT6000).

5-ethynyl-2-deoxyuridine (EdU) assay

Briefly, after different treatments, HUVECs were inoculated in 96-well plates for 48 h. The EDU solution was diluted with cell complete medium at the ratio of 1000:1 to prepare an appropriate amount of 50 μM EDU culture medium. Each well was added 300μL EDU medium and then incubate for 2 h. After cell fixation, Apollo staining, DNA staining, the proliferation activity of cells was observed and detected under fluorescence microscope.

Wound healing assay

First, HUVECs were inoculated in a 6-well plate for 24 h. When the cells were fully fused, the pipette tip was applied to create a scratch wound on the confluent cells in the center. The migration and cell movement of the entire wound area were observed with an inverted optical microscope (Oberkochen, Germany), and the images were taken at 48 h with a camera connected to the microscope (SonyCyber shot, Shanghai Suoguang Visual Products Co., Ltd., China). The cell migration ability was statistically analyzed according to the cell healing.

Transwell assay

HUVECs were firstly adjusted to the appropriate concentration. Subsequently, the upper chamber was added with adjusted cells, whereas the lower chamber was replaced by a medium supplement 15% FBS. After 24 h, 4% paraformaldehyde was used for fixation and 0.1% crystal violet for staining, respectively. Five fields were randomly selected under an inverted microscope to represent the invasion ability of cells in each group.

Measurement of interleukin (IL)-6 AND IL-8 levels by ELISA

The concentrations of IL-6 and IL-8 in the HUVECs and CLP model mice were assessed using a commercially available ELISA kit (USCN Business Co., Ltd, China).

Survival rate analysis

After mice undergoing CLP surgery, the number of mice in each group was observed and counted for survival analysis. The death time and number of these animals were observed and recorded by a researcher who was completely had no knowledge of the study

Hematoxylin-eosin (HE) staining

The aortic tissues were fixed with formaldehyde (10%) for 24 h, and then tissues were placed in a 5% nitric acid decalcification solution for 3–5 d. After washing with water, routine dehydration, transparency, paraffin immersion, embedding and sectioning, the tissue sections were stained with hematoxylin and eosin. Finally, the pathological changes of myocardium tissues were observed under microscope.

Quantitative real-time PCR

TRIpure (Invitrogen, USA) was applied to isolate the sample RNA and PrimeScript RT kit (TaKaRa, Otsu, Japan) was used for reverse transcription. After the RNA was prepared, the expression level was detected with FAST SYBRTM Green Master Mix, and GAPDH was set as internal parameter. 2-ΔΔCt methods represented the fold changes of gene expression and the experiments were conducted three times.

Cell transfection

sh-NC, sh-KCNQ10T1, sh-RNF19A, NC mimic and miR-154-3p mimic and miR-154-3p inhibitor were constructed by Ribobio corporation (Guangzhou, China). When the confluence rate of HUVECs reached 70–80%, the transfection was conducted by using Lipofectamine 2000 (Invitrogen, USA).

Luciferase reporter assay

First, wt-KCNQ10T1, mut-KCNQ10T1, wt-RNF19A and mut-RNF19A were conducted by Quik Change Site-Directed Mutagenesis Kit (AgilentTechnologies). Then, HUVECs were incubated onto 24-well plates and co-transfected with wt-KCNQ10T1 or mut-KCNQ10T1 and wt-RNF19A or mut-RNF19A and miR-154-3p mimic or mimics-NC via Lipofectamine 2000. Finally, the luciferase activity was measured via the Dual-Glo Luciferase Assay System (Promega, USA).

Statistical analysis

All the data were analyzed by SPSS 19.0. One-way ANOVA followed by Dunnett's multiple comparison was applied to assess the differences between the groups. Survival analysis was evaluated by the Kaplan-Meier method. $P < 0.05$ indicated significant difference between groups.

Results

The characteristics of the exosomes extracted from BMMSCs

As shown in Fig. 1A, under TEM, exosomes derived from BMMSCs appeared round or oval in shape. In Fig. 1B, NTA data showed that the average diameter of exosome was 100 nm. Western blot assay revealed positive expression of CD63, CD90 and HSP70 in exosomes (Fig. 1C). These data indicated that the exosomes from BMMSCs were successfully extracted.

Exosomes derived from BMMSCs inhibit LPS-induced proliferation, migration, and invasion of HUVECs

To investigate the uptake and internalization of BMMSCs-derived exosomes into recipient cells, HUVECs were treated with exosomes labeled with PKH26 red fluorescence. After 24 h, we observed that 90% of the exosomes were integrated into the cytoplasm, while in HUVECs labeled directly with PKH26, red fluorescence spread throughout the cell (Fig. 2A). Further, we tested the biological effects of exosomes on HUVECs. Proliferation assays showed that LPS significantly induced the proliferation of HUVECs as comparison to control. In contrast, exosomes treatment resulted in a remarkable reduction in HUVECs activity (Fig. 2B and 2C). Similarly, in the migration and invasion experiments, we found that the exosomes extracted from BMMSCs sharply slowed down the migration and invasion of cells induced by LPS (Fig. 2D and 2E). ELISA results revealed that exosomes reduced the levels of IL-6 and IL-8 in the cell supernatant (Fig. 2F).

Exosomes derived from BMMSCs alleviate sepsis symptoms in CLP model mice

We demonstrated *in vitro* that exosomes inhibited LPS-induced sepsis. To further investigate the therapeutic effect of exosomes on sepsis, we conducted an *in vivo* experiment on CLP model mice. As shown in the survival analysis in Fig. 3A, CLP evidently reduced survival rate in mice. However, when these mice were treated with exosomes, survival rate was significantly increased in model mice. In ELISA, decreased expression of IL-6 and IL-8 was found in the Exos group compared with the CLP group (Fig. 3B). Next, we extracted mouse aortic tissues to evaluate the effect of exosomes on the aortic tissue of CLP mice. HE staining showed that exosomes treatment significantly reduced the necrotic area of the aortic cross-section of CLP mice (Fig. 3C). VEGF was an effective stimulator of endothelial cell permeability, and its elevated level was closely associated with sepsis. Therefore, we extracted aortic endothelial primary cells from CLP model mice to observe the changes of intracellular VEGF. As expected, the protein level of VEGF in Exos group was evidently lower than group CLP (Fig. 3D).

LncRNA-KCNQ1OT1 is involved in the inhibition of sepsis by BMMSCs-derived exosomes

As indicated in Fig. 4, KCNQ1OT1 was evidently lower in aortic endothelial primary cells from the CLP model and LPS-induced HUVECs than in the control group. On the contrary, the expression of KCNQ1OT1 was significantly up-regulated in exosomes, and the level of KCNQ1OT1 in HUVECs was significantly increased when BMMSCs and HUVECs were co-cultured (Fig. 5A and 5B). Further, we compared the expression of KCNQ1OT1 in aortic endothelial primary cells from the CLP model before and after exosomal treatment and found that KCNQ1OT1 was evidently increased in exosomal treated cells (Fig. 5C).

Overexpression of lncRNA-KCNQ1OT1 inhibits LPS-induced proliferation, migration, and invasion of HUVECs

To investigate the role of lncRNA-KCNQ1OT1 in sepsis, we overexpressed KCNQ1OT1. Next, the proliferation activity of HUVECs was detected by CCK8 and EdU assays, and the data showed that KCNQ1OT1 overexpression sharply inhibited LPS-induced cell activity (Fig. 6A and 6B). Meanwhile, we detected the levels of IL-6 and IL-8 in the HUVECs, and observed that these inflammatory cytokines were sharply reduced in the LPS + pc-KCNQ1OT1 group as comparison to the LPS group (Fig. 6C). Furthermore, we examined the effect of pc-KCNQ1OT1 on the migration and invasion of HUVECs. As shown in the wound healing, the cell migration rate of group LPS + pc-KCNQ1OT1 was markedly lower than that of LPS group (Fig. 6D). Similarly, the invasion efficiency of LPS-induced HUVEC cells was significantly inhibited after transfection with pc-KCNQ1OT1 (Fig. 6E).

MiR-154-3p is the target of lncRNA-KCNQ1OT1

To elucidate the molecular mechanism of lncRNA KCNQ1OT1 in regulating the progression of sepsis, we used Starbase to predict its potential targets. As predicted, miR-154-3p was a putative target of KCNQ1OT1 and the binding sites were shown in Fig. 7A. To confirm this speculation, KCNQ1OT1-wt and KCNQ1OT1-mut were used to conduct luciferase reporter assay for verification. As depicted in Fig. 7B, the luciferase activity was significantly inhibited in KCNQ1OT1-wt group, but there was no change in KCNQ1OT1-mut group. Further, we found that the mRNA level of miR-154-3p was sharply up-regulated both in LPS-induced HUVECs and in aortic primary cells extracted from CLP model (Fig. 7C). Besides, the endogenous expression detection of miR-154-3p showed that pc-KCNQ1OT1 evidently inhibited the transcription level of miR-154-3p, confirming that miR-154-3p bound with KCNQ1OT1 (Fig. 7D).

Low expression of miR-154-3p inhibits proliferation, migration and invasion of HUVECs induced by LPS

To explore the role of miR-154-3p in sepsis, we constructed a low expression system of miR-154-3p by adding inhibitors and further detected its effects on cell biological functions. In CCK-8 and EdU assays, compared with LPS-treated HUVECs, the proliferation activity was sharply reduced after the addition of miR-154-3p inhibitor (Fig. 8A and 8B). In ELISA assay, which measured inflammatory cytokine (IL-6 and IL-8) levels, the addition of miR-154-3p inhibitors remarkably decreased the levels of above inflammatory cytokines in the supernatant (Fig. 8C). In migration analysis, the relative wounding width of LPS + miR-154-3p inhibitor group was significantly greater than LPS group after 48-h culture in HUVECs (Fig. 8D). In Transwell assay, the number of invaded HUVECs per field in the LPS + miR-154-3p inhibitor group was significantly lower than that in LPS group (Fig. 8E).

RNF19A is the target of miR-154-3p

To clarify the regulatory mechanism of miR-154-3p in sepsis, we identified differentially expressed genes associated with sepsis via miRWalk, miRDB and ENCORI algorithm and a total of 10 overlapping genes were identified (Fig. 9A). Primers used for Real Time PCR are shown in Table 1. Further quantitative analysis showed that only RNF19A mRNA level was significantly reduced, suggesting that RNF19A might be the target gene of miR-154-3p involved in sepsis (Fig. 9B). The binding sites between miR-154-3p and RNF19A were presented in Fig. 9C. To verify the combination of the two, we carried out luciferase reporter assay and observed that the relative luciferase activity of RNF19A was significantly reduced after transfection with miR-154-3p mimic. However, when this binding site was mutated, over-expression of miR-154-3p did not affect luciferase activity (Fig. 9D). Besides, qRT-PCR results illustrated that transcription levels of RNF19A were remarkably reduced in the septic cell model (Fig. 9E).

Table 1
Primers used for Real Time PCR

Gene Forward (5’-3’) Reserve (3’-5’)		
KCNQ1OT1	CCCAGAAATCCACACCTCGG	TCCTCAGTGAGCAGATGGAGA
miR-154-3p	GTGGTACTTGAAGATAGGTT	TTGGTACTGAAAAATAGGTC
RNF19A	ACTGAACGGTTTAATCCT	CTGTTCCACAGCCTTCTC
ELK4	AACCAGCCTGCACGCGCT	TGCCCATCATTAGAGGTCCAACAG
PSEN1	TATGGCAGAAGGAGACCCG	TATGGCAGAAGGAGACCCG
SP3	CGCAGAAAGTCAGATGCCCT	TGGCTACCAGGCCTATGGAA
PRKRA	ACGAATACGGCATGAAGACC	TGGAAGGGTCAGGCATTAAG
DYRK1A	TCTGGGTATTCCACCTGCTC	GTCCTCCTGTTTCCACTCCA
MOB1B	TTCGGATGGCTGTCATGCTTCC	GCTGACATCACTGGACAACTCTC
PDE10A	GACCTCGCACTGTACTTTG	CTGGCCATAGTTTCGTCAC
TMEM68	GCGAATTCGCCATGATAGATAACAACCAAAC	CAGGATCCATGAGCCTTCTGCTCTTTAT
U6	CTCGCTTCGGCAGCACA	AACGCTTCACGAATTTGCGT
GADPH	GGTGAAGGTCGGTGTGAACG	CTCGCTCCTGGAAGATGGTG

KCNQ1OT1, KCNQ1 opposite strand/antisense transcript 1; RNF19A, ring finger protein 19A; PSEN1, PTEN-induced putative kinase 1; SP3, specificity proteins 3; PRKRA, interferon-inducible double-stranded RNA-dependent protein kinase 20 activator A; MOB1B, Mps one binder kinase activator-like 1B; PDE10A, phosphodiesterase 10A; TMEM68, transmembrane protein.

LncRNA-KCNQ1OT1 inhibits sepsis progression by targeting miR-154-3p/RNF19A

To further explore the interaction relationship between KCNQ1OT1, miR-154-3p and RNF19A in the progression of sepsis, we transfected HUVEC cells with sh-KCNQ1OT1 + NC-ihibitor or sh-KCNQ1OT1 + miR-154-3p inhibitor or sh-KCNQ1OT1 + miR-154-3p inhibitor + sh-RNF19A. As exhibited in Fig. 10A, the proliferation activity of HUVEC cells co-transfected with sh-KCNQ1OT1 + miR-154-3p inhibitor was significantly lower than those transfected with pc-KCNQ1OT1 alone. However, when sh-RNF19A was added, the proliferation activity of HUVEC cells was sharply increased as comparison to sh-KCNQ1OT1 + miR-154-3p inhibitor group (Fig. 10A and 10B). Similarly, the levels of IL-6 and IL-8 in group sh-KCNQ1OT1 + miR-154-3p inhibitor + sh-RNF19A were significantly higher than those in group sh-KCNQ1OT1 + miR-154-3p inhibitor (Fig. 10C). In cell metastasis assays (wound healing and transwell), we still observed the same expression pattern, that is, transfection sh-KCNQ1OT1 + miR-154-3p inhibitor + sh-RNF19A increased the ability of cell migration and invasion compared with transfection sh-KCNQ1OT1 + miR-154-3p inhibitor (Fig. 10D and 10E).

Discussion

When the polycystic body fuses with the plasma membrane into the extracellular space, exosomes from the endosomal membrane are released [18]. Exosomes are uniform in size, usually between 50 nm and 150 nm [19]. In addition, In addition, exosomes can be used as therapeutics because they can express specific marker proteins [20]. Typically, these markers play a vital role in intracellular formation and transport as well as target cell recognition. In the current study, we extracted exosomes from BMMSC successfully. The exosomes were round or oval in shape, with an average size of about 100nm, and expressed positive surface marker antigens such as CD63, CD81 and HSP70. Recently, exosomes have received widespread attention due to their extensive participation in the progression of various diseases, such as inflammation, tumorigenesis, and angiogenesis [21, 22]. In our research, we confirmed that BMMSC-derived exosomes significantly reduced sepsis toxicity and alleviated sepsis symptoms through *in vivo* and *in vitro* experiments. Sepsis is characterized by severe cytokine storms, in which large amounts of proinflammatory cytokines can be detected in the bloodstream [4]. Consistently, our results showed that exosomes significantly reduced pro-inflammatory cytokines in the supernatant.

Recently, it has been reported that exosomes from BMMSCs affected cell proliferation and survival through the transport of lncRNAs [3]. Moreover, lncRNAs have been proved to be novel gene regulators and prognostic markers for sepsis [23]. Therefore, to explore the mechanism of lncRNAs in sepsis was conducive to finding an effective therapeutic target. It was reported that KCNQ1OT1 was related to many diseases and abnormally expressed in various diseases. Jiang *et al.* have revealed that silencing KCNQ1OT1 expression regulates QT interval prolongation [24]. Hu *et al.* have found that KCNQ1OT1 up-regulates the expression of ABCC1, thereby increasing the chemotherapy resistance of oxaliplatin to hepatocellular carcinoma [25]. In addition, KCNQ1OT1 is an important prognostic marker in diabetic retinopathy, osteolysis and other diseases [26, 27]. However, the mechanism of KCNQ1OT1 in sepsis had not been fully elucidated. In present study, we found that KCNQ1OT1 expression was low in the sepsis model, and overall survival was relatively low. On the contrary, it was highly expressed in exosomes. More notably, HUVECs and BMMSCs co-transfection significantly up-regulated KCNQ1OT1 expression. Further functional studies showed that over-expression of KCNQ1OT1 inhibited LPS-induced cell proliferation, metastasis, and inflammatory response. Taken together, our data indicated that BMMSCs-derived exosomal KCNQ10T1 inhibited the progression of sepsis.

MicroRNAs (miRNAs) are small non-protein coding RNA molecules [28]. Since they play an important role in the regulation of proliferation, survival, apoptosis and other biological processes, the abnormal expression of miRNAs is associated with the occurrence and development of many diseases [29, 30]. Previously, data has revealed that miR-154-3p is used as a tumor suppressor and an effective target for the treatment of breast cancer [31]. Another study has also shown that miR-154-3p was significantly down-regulated in ductal carcinoma in situ [32]. Besides, miR-154-3p has been reported in papillary thyroid carcinoma, which promoted the deterioration of papillary thyroid carcinoma [33]. However, there were few studies on the role of miR-154-3p in sepsis, let alone its deeper regulatory mechanism. In this study, miR-154-3p was sharply up-regulated in the sepsis model as a downstream target of KCNQ1OT1. Further functional studies showed that low expression of miR-154-3p evidently inhibited LPS-induced cell proliferation, metastasis, and inflammatory response. Collectively, we confirmed that KCNQ1OT1 acted as a sponge for miR-154-3p in the regulation of sepsis progression.

RNF19A, also known as Dorfin, which has ubiquitin ligase activity [34]. Besides, RNF19A has affinity for ubiquitin-conjugating enzymes [35]. It has been reported that RNF19A is expressed in many organs, such as the kidney, liver, intestine and central nervous system [36]. A previous study shows that RNF19A is related to familial amyotrophic lateral sclerosis and Parkinson's disease, and inhibits neurophenotype and motor neuron death [37]. Besides, RNF19a has been shown to be involved in sperm cell head formation, head-to-tail coupling, and tail development [38]. In our study, we confirmed that RNF19A was significantly down-regulated in the sepsis model and that RNF19A was the downstream target gene of miR-154-3p involved in sepsis. Moreover, the rescue experiment suggested that KCNQ10T1 inhibited sepsis progression by targeting the miR-154-3p/RNF19A axis.

Conclusions

In this study, we mainly explored the functionality of BMMSCs-derived exosomal KCNQ10T1 and its potential interactions with miR-154-3p/RNF19A axis in sepsis. We found that KCNQ10T1 was down-regulated in sepsis model and might regulate miR-154-3p/RNF19A axis to participate in the regulation of sepsis progression.

Abbreviations

Abbreviations	Original words
BMMSCs	bone marrow mesenchymal stem cells
CCK-8	Cell Counting Kit-8
CLP	Cecal ligation puncture
EdU	5-ethynyl-2-deoxyuridine
HE	Hematoxylin-eosin
HUVECs	Human Umbilical Vein Endothelial Cells
IL	interleukin
KCNQ1OT1	KCNQ1 opposite strand/antisense transcript 1
lncRNAs	Long non-coding RNAs
LPS	ipopolysaccharide
NTA	nanoparticle tracking analysis
QRT-PCR	Quantitative real-time PCR
TEM	transmission electron microscopy

Declarations

Ethics approval and consent to participate

The experimental protocol was approved by the Animal Ethics Committee of Nantong University.

Availability of data and materials

All data generated or analyzed during this study are included in this published article.

Consent for publication

Not applicable.

Competing interests

The authors state that there are no conflicts of interest.

Funding

This work was supported by the Science and Technology Project of Nantong City (MSZ20079 and JC2021024), Science and Technology Project of Nantong Municipal Health Commission (MA2020023) and Social Science Foundation of Jiangsu Province (19JYD008).

Authors’ Contributions

HJY and JBY conceived and designed the study. CL conducted most of the experiments. JJL analyzed the data. JHX performed the literature search and data extraction. YY drafted the manuscript. HYZ and YY finalized the manuscript. All authors read and approved the final manuscript.

Acknowledgements

We deeply appreciate the supports by all participants.

References

1. Alkharfy KM, Ahmad A, Jan BL, Raish M: **Thymoquinone reduces mortality and suppresses early acute inflammatory markers of sepsis in a mouse model**. Biomed Pharmacother 2018, **98**:801–805.
2. Seymour CW, Cooke CR, Heckbert SR, Spertus JA, Callaway CW, Martin-Gill C, Yealy DM, Rea TD, Angus DC: **Prehospital intravenous access and fluid resuscitation in severe sepsis: an observational cohort study**. Crit Care 2014, **18**(5):533.
3. Yong H, Wu G, Chen J, Liu X, Bai Y, Tang N, Liu L, Wei J: **lncRNA MALAT1 Accelerates Skeletal Muscle Cell Apoptosis and Inflammatory Response in Sepsis by Decreasing BRCA1 Expression by Recruiting EZH2**. Mol Ther Nucleic Acids 2020, **21**:1120–1121.
4. Essandoh K, Yang L, Wang X, Huang W, Qin D, Hao J, Wang Y, Zingarelli B, Peng T, Fan GC: **Blockade of exosome generation with GW4869 dampens the sepsis-induced inflammation and cardiac dysfunction**. Biochim Biophys Acta 2015, **1852**(11):2362–2371.
5. Boyd JH, Forbes J, Nakada TA, Walley KR, Russell JA: **Fluid resuscitation in septic shock: a positive fluid balance and elevated central venous pressure are associated with increased mortality**. Crit Care Med 2011, **39**(2):259–265.
6. Chen Q, Liu Y, Ding X, Li Q, Qiu F, Wang M, Shen Z, Zheng H, Fu G: **Bone marrow mesenchymal stem cell-secreted exosomes carrying microRNA-125b protect against myocardial ischemia reperfusion injury via targeting SIRT7**. Mol Cell Biochem 2020, **465**(1–2):103–114.
7. Shen ZY, Zhang J, Song HL, Zheng WP: **Bone-marrow mesenchymal stem cells reduce rat intestinal ischemia-reperfusion injury, ZO-1 downregulation and tight junction disruption via a TNF-alpha-regulated mechanism**. World J Gastroenterol 2013, **19**(23):3583–3595.
8. Le Blanc K, Tammik C, Rosendahl K, Zetterberg E, Ringden O: **HLA expression and immunologic properties of differentiated and undifferentiated mesenchymal stem cells**. Exp Hematol 2003, **31**(10):890–896.
9. Borger V, Bremer M, Ferrer-Tur R, Gockeln L, Stambouli O, Becic A, Giebel B: **Mesenchymal Stem/Stromal Cell-Derived Extracellular Vesicles and Their Potential as Novel Immunomodulatory Therapeutic Agents**. Int J Mol Sci 2017, **18**(7).
10. Phinney DG, Di Giuseppe M, Njah J, Sala E, Shiva S, St Croix CM, Stolz DB, Watkins SC, Di YP, Leikauf GD *et al*: **Mesenchymal stem cells use extracellular vesicles to outsource mitophagy and shuttle**

microRNAs. Nat Commun 2015, **6**:8472.

11. Kim DK, Nishida H, An SY, Shetty AK, Bartosh TJ, Prockop DJ: **Chromatographically isolated CD63 + CD81 + extracellular vesicles from mesenchymal stromal cells rescue cognitive impairments after TBI**. Proc Natl Acad Sci U S A 2016, **113**(1):170–175.
12. Dey BK, Mueller AC, Dutta A: **Long non-coding RNAs as emerging regulators of differentiation, development, and disease**. Transcription 2014, **5**(4):e944014.
13. Yang F, Qin Y, Wang Y, Li A, Lv J, Sun X, Che H, Han T, Meng S, Bai Y *et al*: **LncRNA KCNQ1OT1 Mediates Pyroptosis in Diabetic Cardiomyopathy**. Cell Physiol Biochem 2018, **50**(4):1230–1244.
14. Wu H, Liu J, Li W, Liu G, Li Z: **LncRNA-HOTAIR promotes TNF-alpha production in cardiomyocytes of LPS-induced sepsis mice by activating NF-kappaB pathway**. Biochem Biophys Res Commun 2016, **471**(1):240–246.
15. Kanduri C: **Kcnq1ot1: a chromatin regulatory RNA**. Semin Cell Dev Biol 2011, **22**(4):343–350.
16. Li X, Dai Y, Yan S, Shi Y, Han B, Li J, Cha L, Mu J: **Down-regulation of lncRNA KCNQ1OT1 protects against myocardial ischemia/reperfusion injury following acute myocardial infarction**. Biochem Biophys Res Commun 2017, **491**(4):1026–1033.
17. Sun H, Li Y, Kong H, Dai S, Qian H: **Dysregulation of KCNQ1OT1 promotes cholangiocarcinoma progression via miR-140-5p/SOX4 axis**. Arch Biochem Biophys 2018, **658**:7–15.
18. Gyorgy B, Szabo TG, Pasztoi M, Pal Z, Misjak P, Aradi B, Laszlo V, Pallinger E, Pap E, Kittel A *et al*: **Membrane vesicles, current state-of-the-art: emerging role of extracellular vesicles**. Cell Mol Life Sci 2011, **68**(16):2667–2688.
19. Niu Z, Pang RTK, Liu W, Li Q, Cheng R, Yeung WSB: **Polymer-based precipitation preserves biological activities of extracellular vesicles from an endometrial cell line**. PLoS One 2017, **12**(10):e0186534.
20. Andreu Z, Yanez-Mo M: **Tetraspanins in extracellular vesicle formation and function**. Front Immunol 2014, **5**:442.
21. Wang X, Huang W, Liu G, Cai W, Millard RW, Wang Y, Chang J, Peng T, Fan GC: **Cardiomyocytes mediate anti-angiogenesis in type 2 diabetic rats through the exosomal transfer of miR-320 into endothelial cells**. J Mol Cell Cardiol 2014, **74**:139–150.
22. Ailawadi S, Wang X, Gu H, Fan GC: **Pathologic function and therapeutic potential of exosomes in cardiovascular disease**. Biochim Biophys Acta 2015, **1852**(1):1–11.
23. Jiang Y, Du W, Chu Q, Qin Y, Tuguzbaeva G, Wang H, Li A, Li G, Li Y, Chai L *et al*: **Downregulation of Long Non-Coding RNA Kcnq1ot1: An Important Mechanism of Arsenic Trioxide-Induced Long QT Syndrome**. Cell Physiol Biochem 2018, **45**(1):192–202.
24. Hu H, Yang L, Li L, Zeng C: **Long non-coding RNA KCNQ1OT1 modulates oxaliplatin resistance in hepatocellular carcinoma through miR-7-5p/ ABCC1 axis**. Biochem Biophys Res Commun 2018, **503**(4):2400–2406.
25. Sun X, Xin Y, Wang M, Li S, Miao S, Xuan Y, Wang Y, Lu T, Liu J, Jiao W: **Overexpression of long non-coding RNA KCNQ1OT1 is related to good prognosis via inhibiting cell proliferation in non-small cell lung cancer**. Thorac Cancer 2018, **9**(5):523–531.

26. Shao J, Pan X, Yin X, Fan G, Tan C, Yao Y, Xin Y, Sun C: **KCNQ1OT1 affects the progression of diabetic retinopathy by regulating miR-1470 and epidermal growth factor receptor**. J Cell Physiol 2019, **234**(10):17269–17279.
27. Bartel DP: **MicroRNAs: genomics, biogenesis, mechanism, and function**. Cell 2004, **116**(2):281–297.
28. Cheng CJ, Bahal R, Babar IA, Pincus Z, Barrera F, Liu C, Svoronos A, Braddock DT, Glazer PM, Engelman DM *et al*: **MicroRNA silencing for cancer therapy targeted to the tumour microenvironment**. Nature 2015, **518**(7537):107–110.
29. Chen H, Liu X, Jin Z, Gou C, Liang M, Cui L, Zhao X: **A three miRNAs signature for predicting the transformation of oral leukoplakia to oral squamous cell carcinoma**. Am J Cancer Res 2018, **8**(8):1403–1413.
30. Xu H, Fei D, Zong S, Fan Z: **MicroRNA-154 inhibits growth and invasion of breast cancer cells through targeting E2F5**. Am J Transl Res 2016, **8**(6):2620–2630.
31. Li S, Meng H, Zhou F, Zhai L, Zhang L, Gu F, Fan Y, Lang R, Fu L, Gu L *et al*: **MicroRNA-132 is frequently down-regulated in ductal carcinoma in situ (DCIS) of breast and acts as a tumor suppressor by inhibiting cell proliferation**. Pathol Res Pract 2013, **209**(3):179–183.
32. Ma J, Kan Z: **Circular RNA circ_0008274 enhances the malignant progression of papillary thyroid carcinoma via modulating solute carrier family 7 member 11 by sponging miR-154-3p**. *Endocr J* 2021, **68**(5):543–552.
33. Takeuchi H, Niwa J, Hishikawa N, Ishigaki S, Tanaka F, Doyu M, Sobue G: **Dorfin prevents cell death by reducing mitochondrial localizing mutant superoxide dismutase 1 in a neuronal cell model of familial amyotrophic lateral sclerosis**. J Neurochem 2004, **89**(1):64–72.
34. Park H, Yang J, Kim R, Li Y, Lee Y, Lee C, Park J, Lee D, Kim H, Kim E: **Mice lacking the PSD-95-interacting E3 ligase, Dorfin/Rnf19a, display reduced adult neurogenesis, enhanced long-term potentiation, and impaired contextual fear conditioning**. Sci Rep 2015, **5**:16410.
35. Huang Y, Niwa J, Sobue G, Breitwieser GE: **Calcium-sensing receptor ubiquitination and degradation mediated by the E3 ubiquitin ligase dorfin**. J Biol Chem 2006, **281**(17):11610–11617.
36. Sone J, Niwa J, Kawai K, Ishigaki S, Yamada S, Adachi H, Katsuno M, Tanaka F, Doyu M, Sobue G: **Dorfin ameliorates phenotypes in a transgenic mouse model of amyotrophic lateral sclerosis**. J Neurosci Res 2010, **88**(1):123–135.
37. Rivkin E, Kierszenbaum AL, Gil M, Tres LL: **Rnf19a, a ubiquitin protein ligase, and Psmc3, a component of the 26S proteasome, tether to the acrosome membranes and the head-tail coupling apparatus during rat spermatid development**. Dev Dyn 2009, **238**(7):1851–1861.
38. Ho J, Chan H, Wong SH, Wang MH, Yu J, Xiao Z, Liu X, Choi G, Leung CC, Wong WT *et al*: **The involvement of regulatory non-coding RNAs in sepsis: a systematic review**. Crit Care 2016, **20**(1):383.

Figures

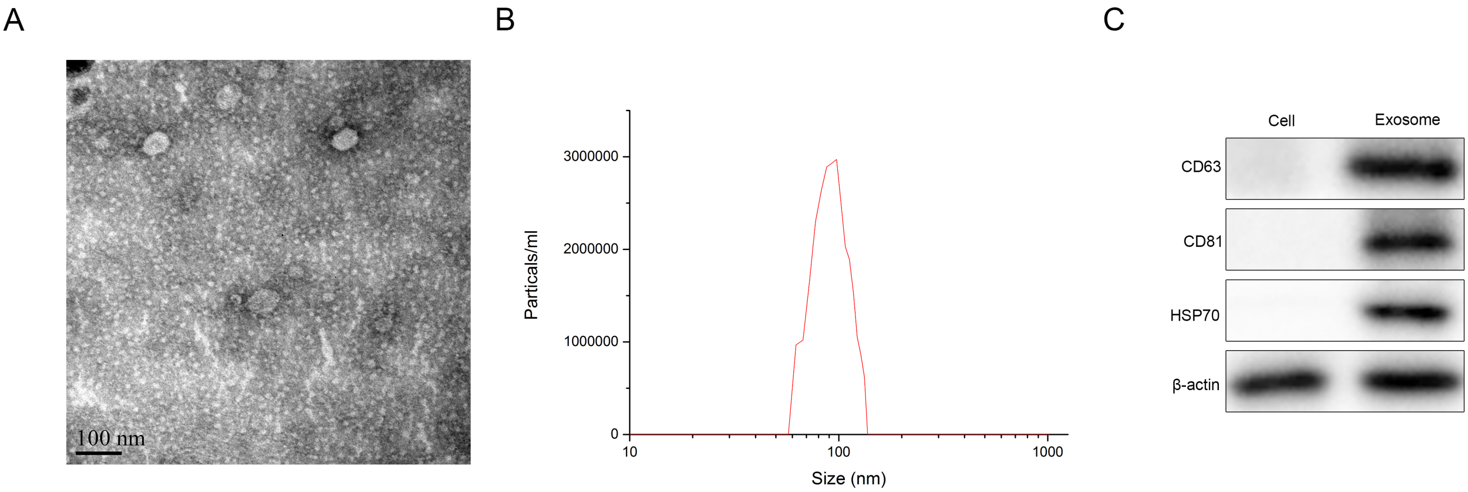

Figure 1

The characteristics of the exosomes extracted from BMMSCs. A) TEM was applied to observe the morphology of exosomes extracted from BMMSCs; B) NTA was used to analyze the size distribution of the extracted exosomes; C) Western blot was conducted to detect the surface antigens CD63, CD90 and HSP70 in exosomes.

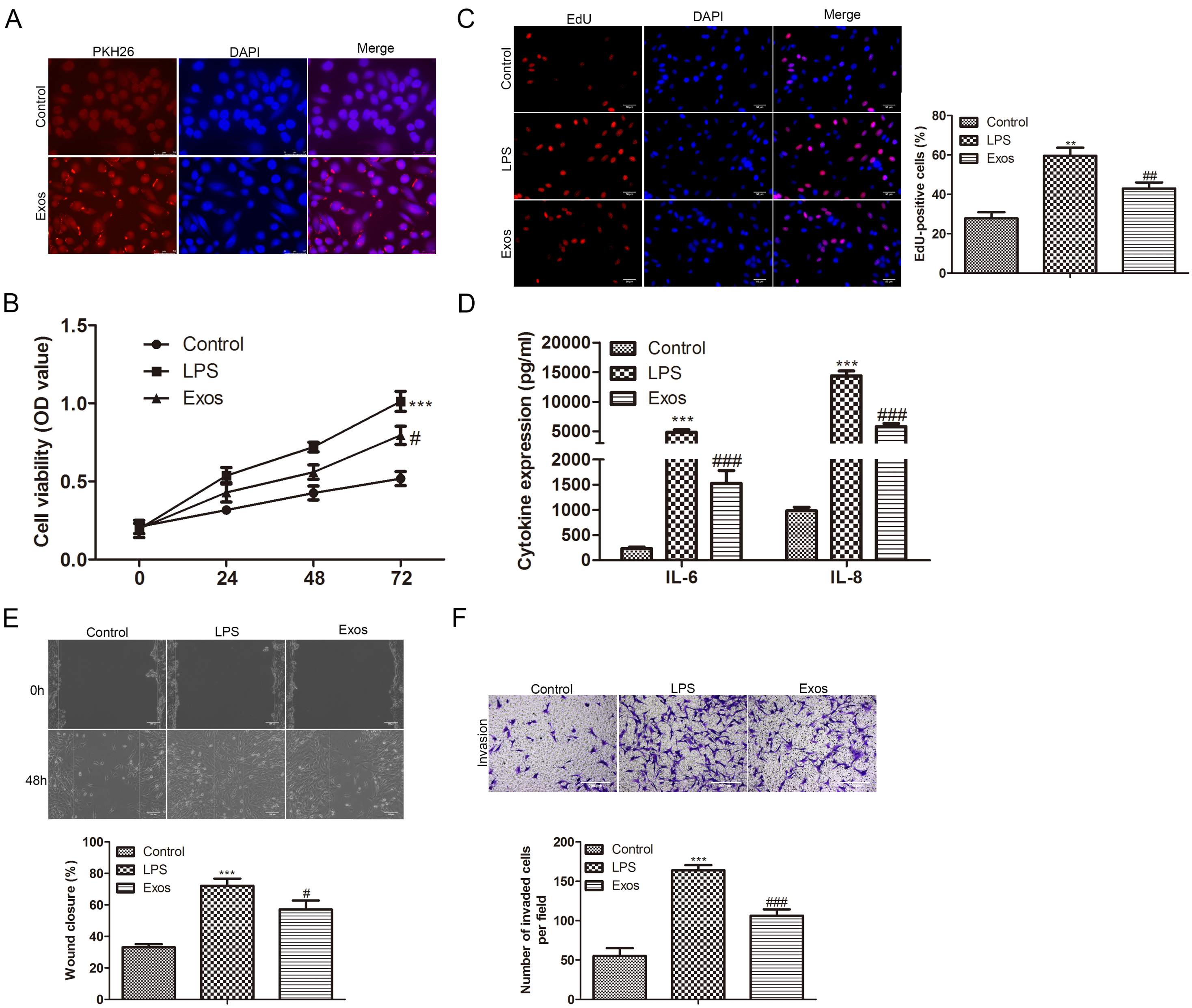

Figure 2

Exosomes derived from BMMSCs inhibit LPS-induced proliferation, migration, and invasion of HUVECs. A) Fluorescence labeling was used to detect the internalization of exosomes in HUVECs; The proliferation activity of HUVECs in the control, the LPS and the Exos groups was observed by B) CCK-8 and C) EdU; The migration and invasion of HUVECs in the control, the LPS and the Exos groups was evaluated by D) wound healing and E) Transwell; F) ELISA was conducted to test the levels of IL-6 and IL-8 in the cell supernatant.

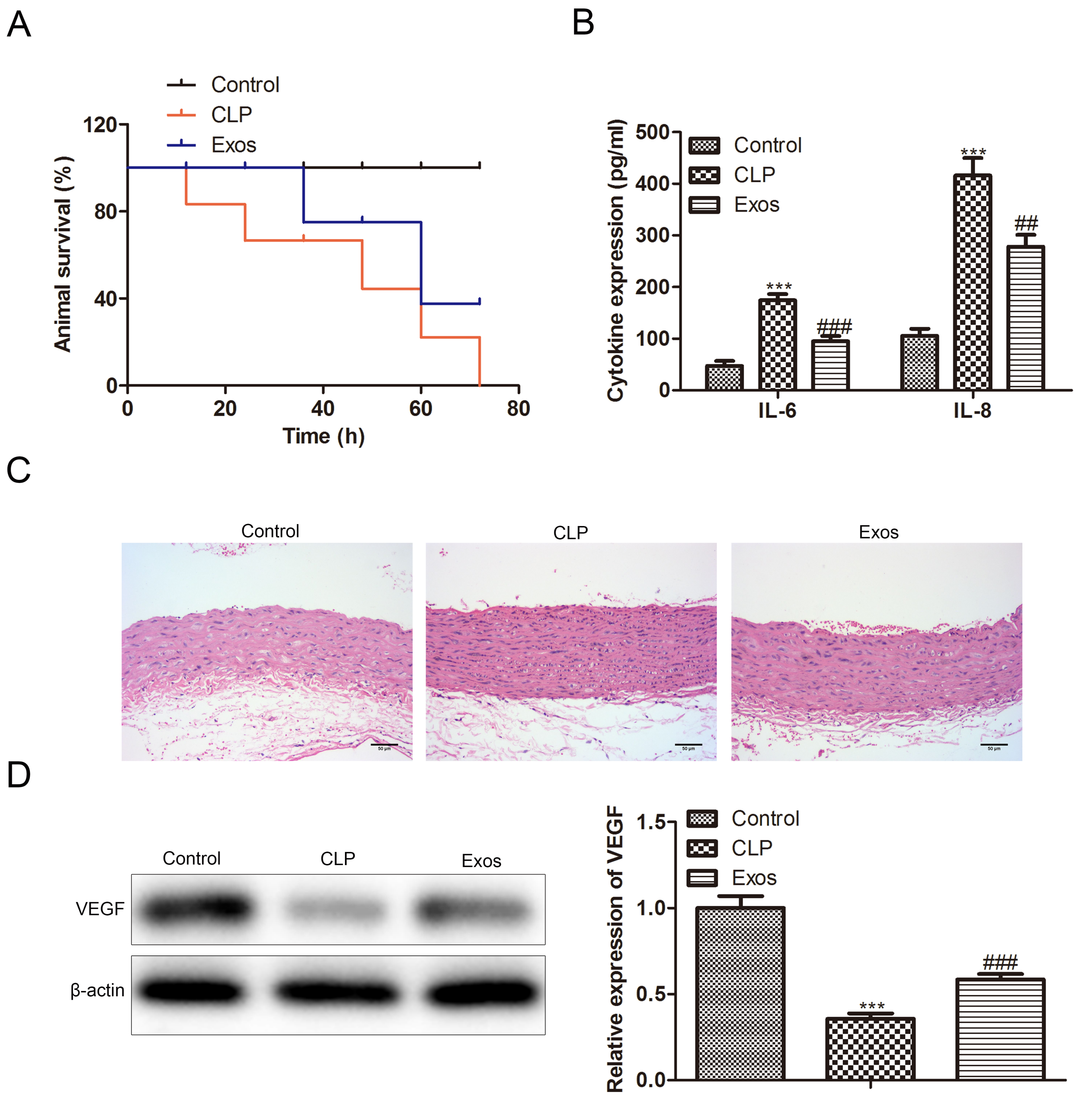

Figure 3

Exosomes derived from BMMSCs alleviate sepsis symptoms in CLP model mice. A) Survival rate analysis of different groups of animals; B) The levels of IL-6 and IL-8 in the cell supernatant was evaluated by ELISA; C) The area of cross-sectional aortic necrosis in CLP mice was identified by HE staining; D) Western Blot was applied to quantitatively analyze the protein expression of VEGF in different groups.

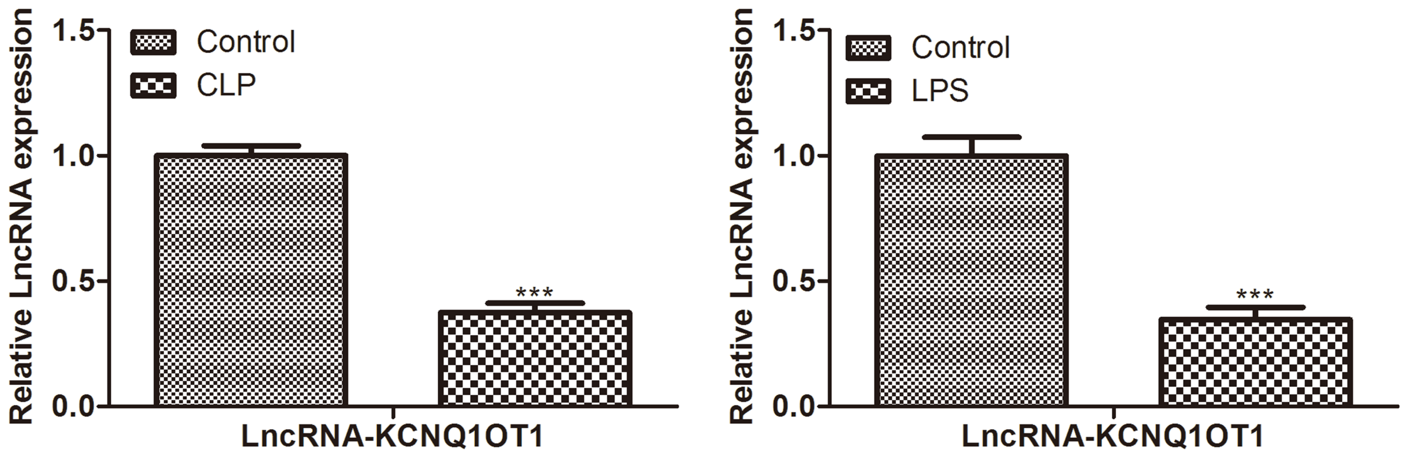

Figure 4

BMMSCs-derived exosomes inhibit sepsis through lncRNA-KCNQ1OT1. The transcriptional activity of KCNQ1OT1 in the sepsis cell model was detected.

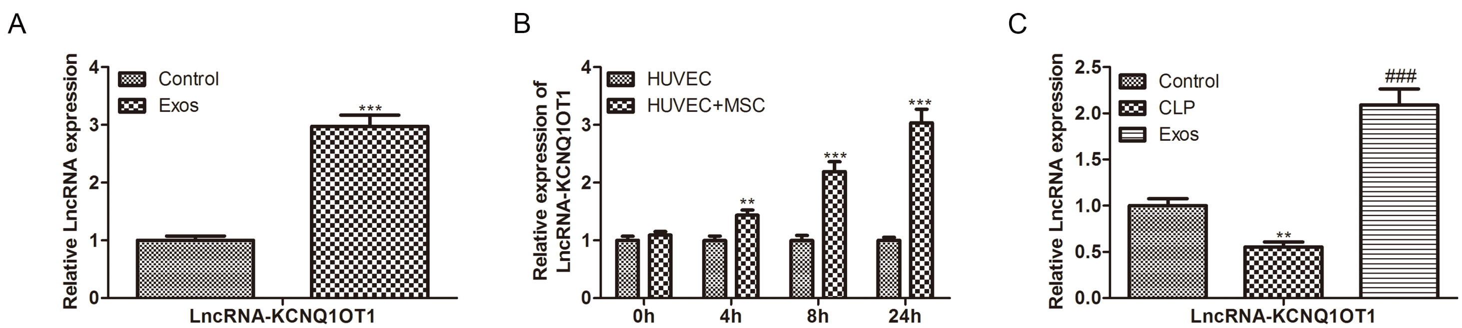

Figure 5

LncRNA-KCNQ1OT1 is involved in the inhibition of sepsis by BMMSCs-derived exosomes. A) The transcriptional activity of KCNQ1OT1 in the control group and Exos group was detected; B) The transcriptional activity of KCNQ1OT1 in the HUVECs group and HUVECs + MSC group was detected; C) The transcriptional activity of KCNQ1OT1 in the control group, CLP group and Exos group was detected.

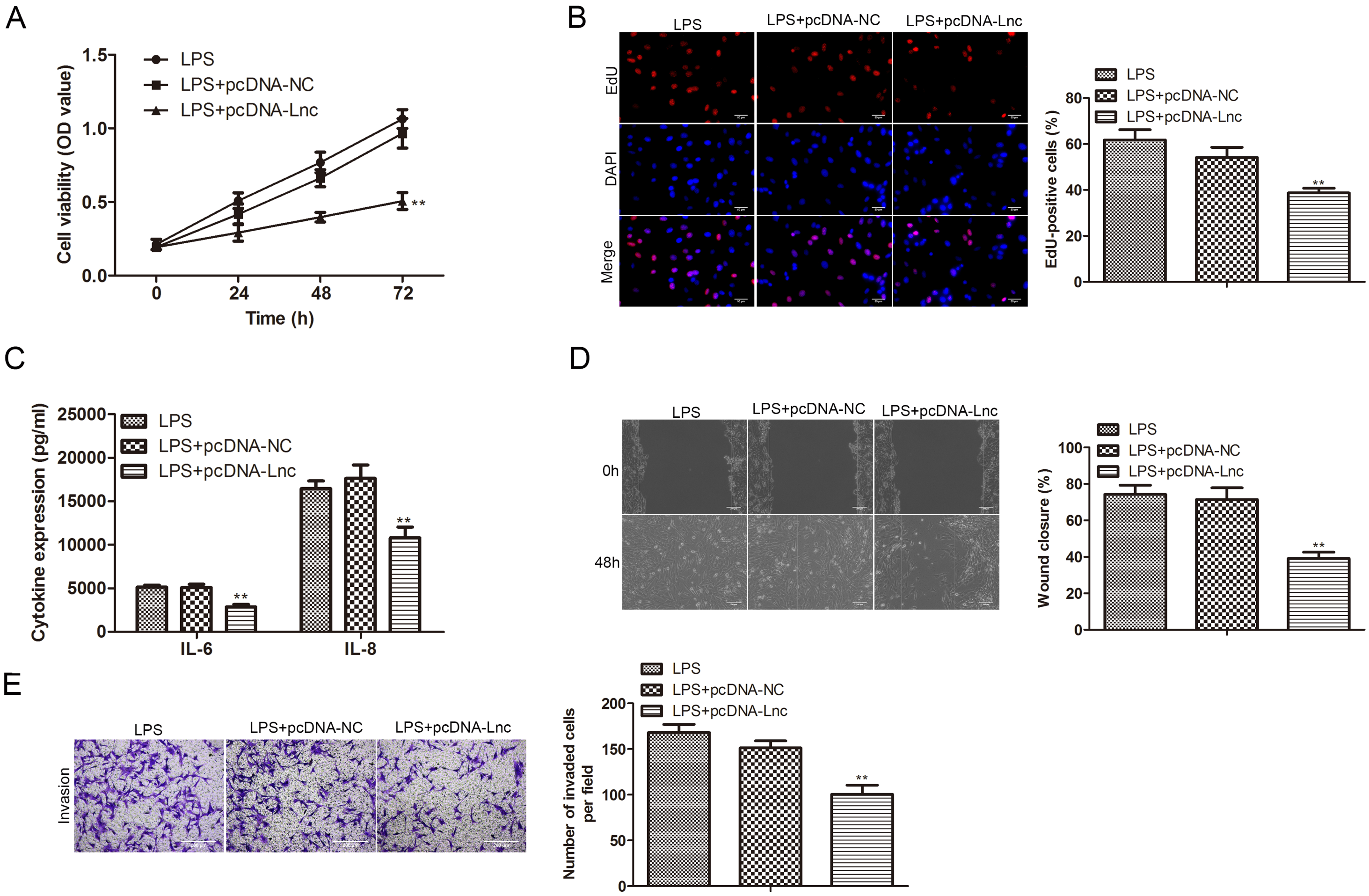

Figure 6

Over-expression of lncRNA-KCNQ1OT1 inhibites LPS-induced proliferation, migration and invasion of HUVECs. After transfection with pc-KCNQ1OT1, the proliferation ability of LPS-induced HUVECs was measured by A) CCK-8 and B) EdU; C) The levels of IL-6 and IL-8 in the cell supernatant was determined by ELISA after transfection with pc-KCNQ1OT1; After transfection with pc-KCNQ1OT1, the migration ability and invasion ability of LPS-induced HUVECs was measured by D) wound healing and E) transwell.

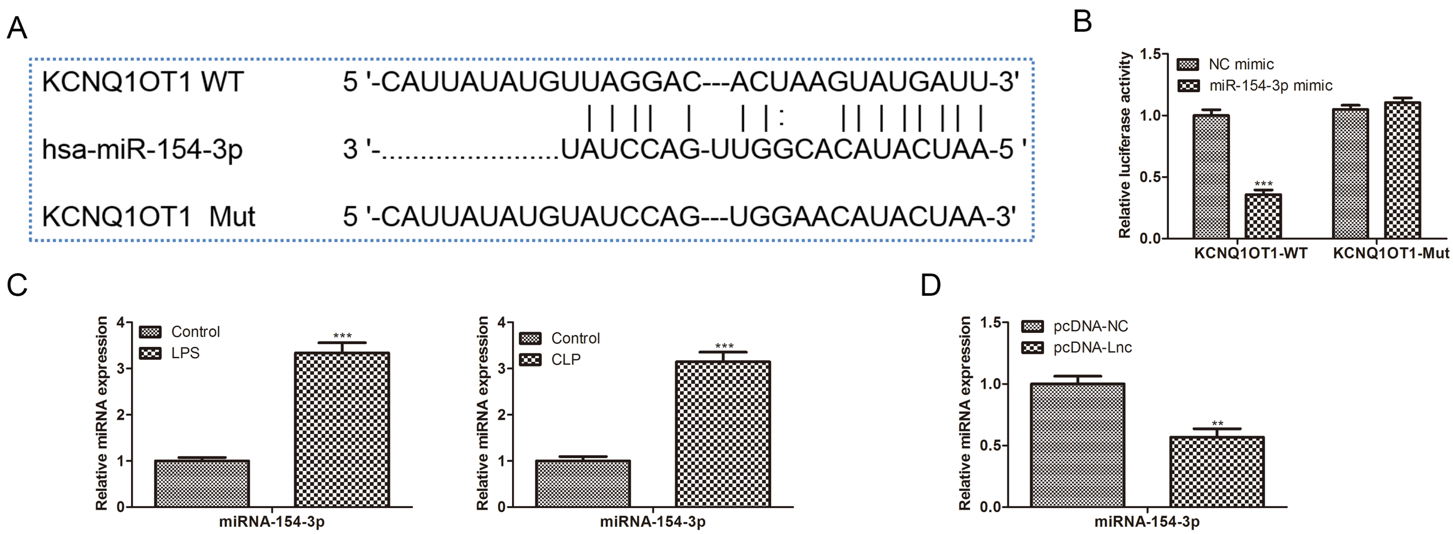

Figure 7

MiR-154-3p was the target of lncRNA-KCNQ1OT1. A) The complementary binding region; B) KCNQ1OT1-wt or KCNQ1OT1-mut were co-transfection with miR-154-3p, then the luciferase activity was evaluated; C) The miR-154-3p expression in control group and cell model of sepsis (LPS-induced HUVECs and mouse aortic endothelial primary cells from CLP model) were detected; D) MiR-154-3p mRNA expression in pc-KCNQ1OT1 group was examined by RT-qPCR.

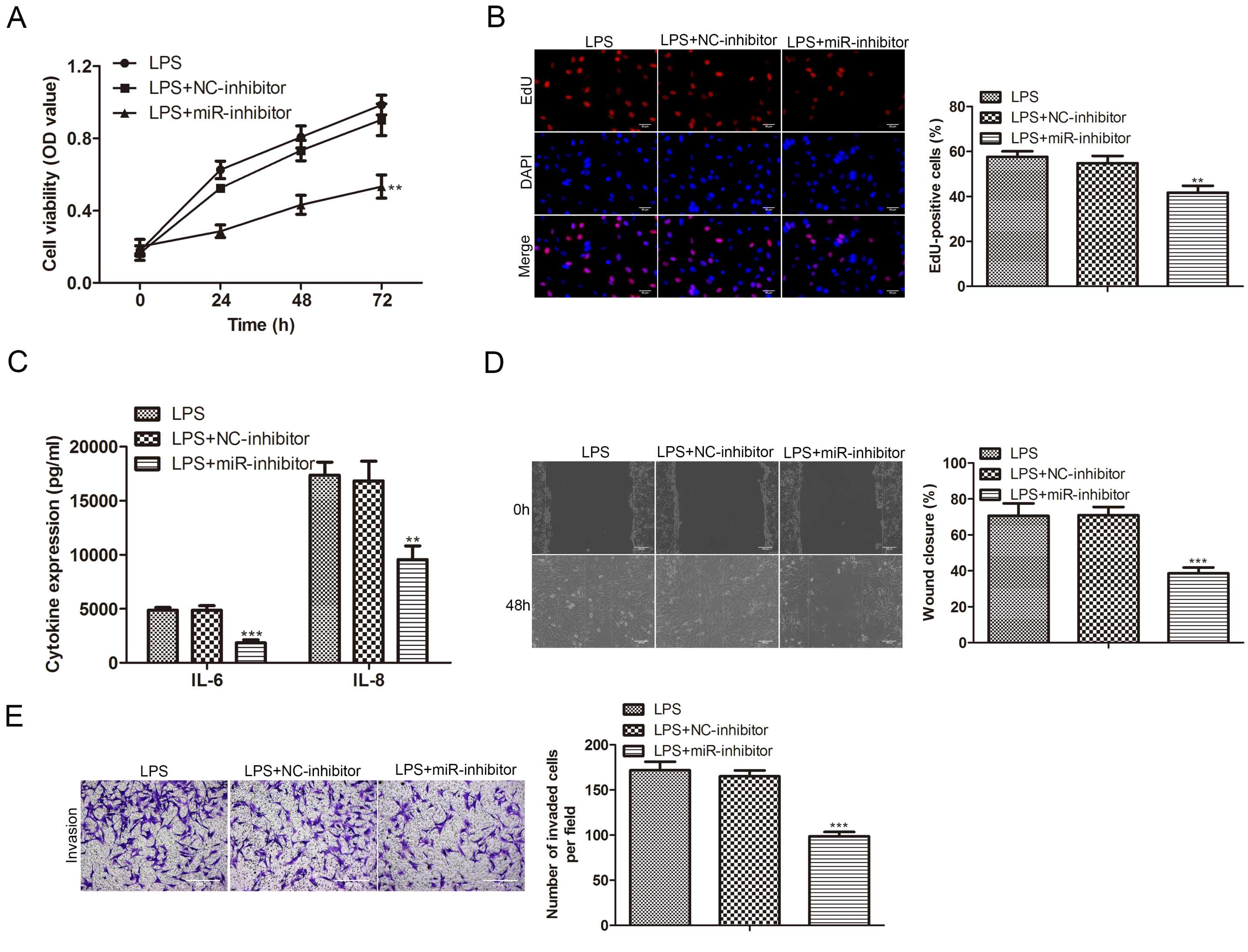

Figure 8

Low expression of miR-154-3p inhibited proliferation, migration and invasion of HUVECs induced by LPS. After the addition of miR-154-3p inhibitor, the proliferation ability of LPS-induced HUVECs was measured by A) CCK-8 and B) EdU; C) The levels of IL-6 and IL-8 in the cell supernatant was determined by ELISA after the addition of miR-154-3p inhibitor; After the addition of miR-154-3p inhibitor, the migration ability and invasion ability of LPS-induced HUVECs was measured by D) wound healing and E) transwell.

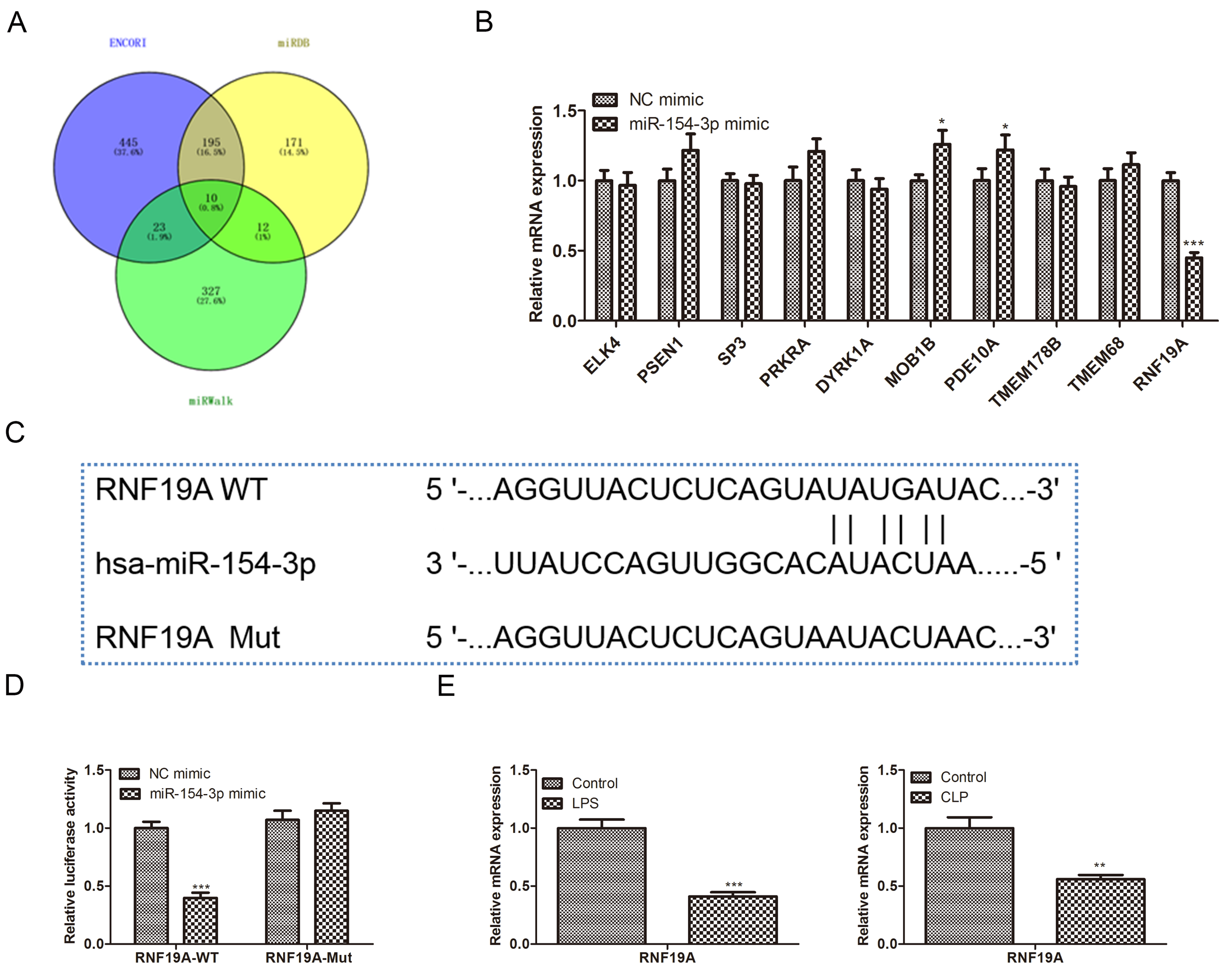

Figure 9

RNF19A was the target of miR-154-3p. A) miRwalk, miRDB and ENCORI were used to predict the target; B) The mRNA levels of the screened target genes were quantitatively detected by RT-qPCR; C) The binding site between miR-154-3p and RNF19A; D) RNF19A-wt or RNF19A-mut were co-transfection with miR-154-3p mimic, then the relative luciferase activity was evaluated; E) RNF19A mRNA expression in control group and cell model of sepsis (LPS-induced HUVECs and mouse aortic endothelial primary cells from CLP model) was examined by RT-qPCR.

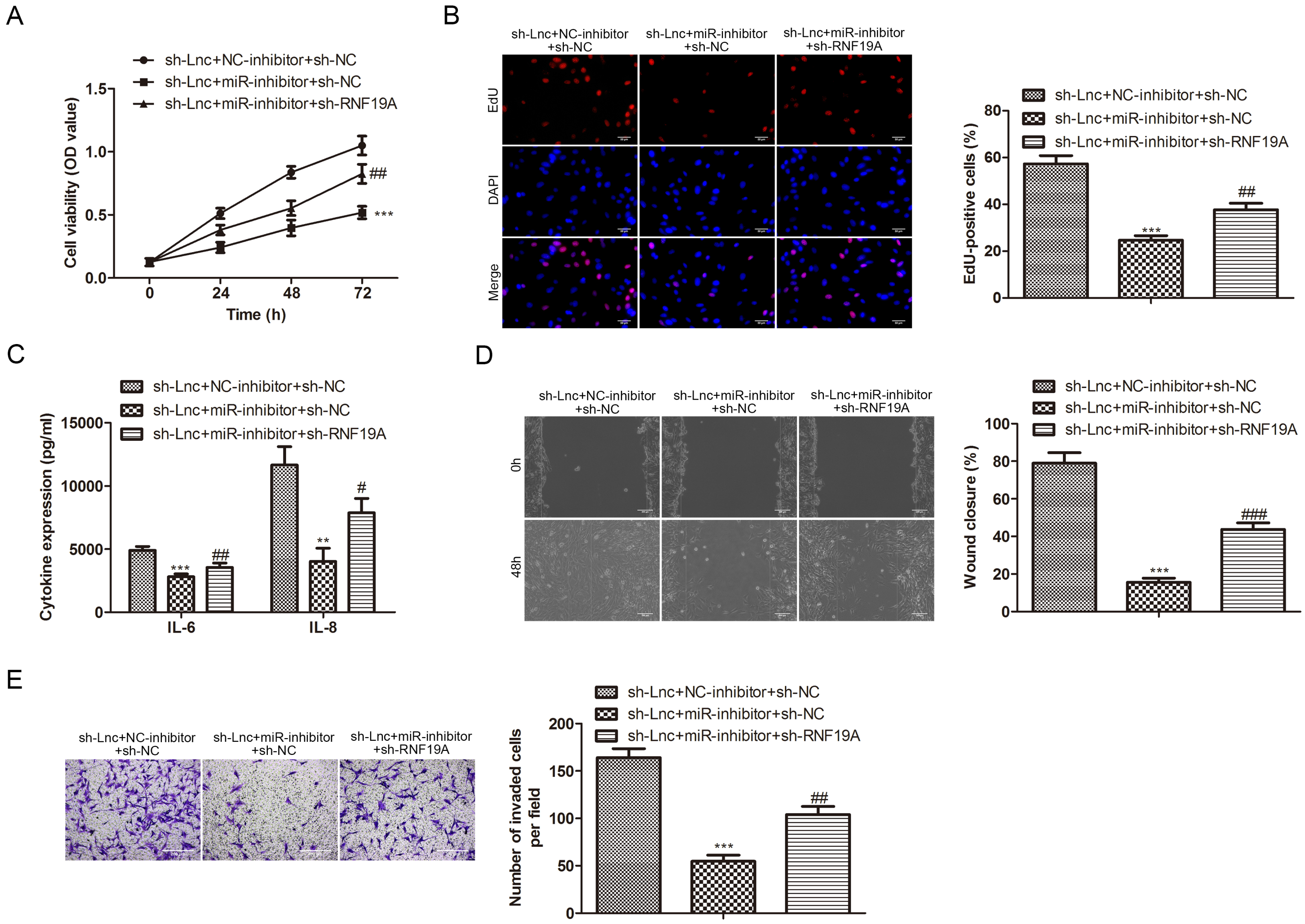

Figure 10

LncRNA-KCNQ1OT1 inhibits sepsis progression by targeting miR-154-3p/RNF19A. The proliferation ability of LPS-induced HUVECs in indicated groups was measured by A) CCK-8 and B) EdU; C) The levels of IL-6 and IL-8 in the cell supernatant was determined by ELISA; The migration ability and invasion ability of LPS-induced HUVECs in indicated groups was measured by D) wound healing and E) Transwell.